

# Unified moisture algorithm for improved RF dielectric grain moisture measurement

David B Funk<sup>1</sup>, Zoltan Gillay<sup>2</sup> and Peter Meszaros<sup>2</sup>

<sup>1</sup> US Department of Agriculture—Grain Inspection, Packers and Stockyards Administration, 10383 N Ambassador Dr., Kansas City, MO 64153, USA

<sup>2</sup> Faculty of Food Science, Corvinus University of Budapest, 14-16 Somloi ut, 1118 Budapest, Hungary

E-mail: [david.b.funk@usda.gov](mailto:david.b.funk@usda.gov), [zoltan.gillay@uni-corvinus.hu](mailto:zoltan.gillay@uni-corvinus.hu) and [peter.meszaros@uni-corvinus.hu](mailto:peter.meszaros@uni-corvinus.hu)

Received 31 May 2006, in final form 4 August 2006

Published 27 February 2007

Online at [stacks.iop.org/MST/18/1004](http://stacks.iop.org/MST/18/1004)

## Abstract

This paper presents a Unified Grain Moisture Algorithm based on measurements of the real part of the complex permittivity of grain at 149 MHz. The main goal of the method was to enable different moisture meter models to provide equivalent moisture predictions without calibration development. The database that was used to create and test the method included 6189 grain samples representing 53 grain types of US grain that were collected over a period of 6 years. The overall standard deviation of differences with respect to the air-oven method was 0.34% moisture. Methods for transferring grain moisture calibrations from the original ‘Master’ test cell to a smaller test cell were developed and tested. Three temperature correction functions with differing levels of complexity were evaluated. The algorithm is available as a public algorithm for commercialization by multiple manufacturers.

**Keywords:** radio-frequency, moisture, grain, dielectric, unified calibration, transfer, temperature correction

## 1. Introduction

Moisture content is one of the most important quality factors in marketing grain, since it determines both the quantity of dry matter traded and the storability of the grain. Grain moisture meters based on the RF dielectric method have been used widely for over 50 years because the technique is capable of reasonably good accuracy for all grain types (with appropriate calibrations), the time required for a measurement is compatible with grain producers’ and handlers’ needs, and the cost of the instrumentation is moderate. However, the RF dielectric method has been hampered by calibration cost and complexity associated with differences between grain types and differences from year to year for specific grain types. Furthermore, the lack of standardization of measurement frequency and sensing technology has severely limited calibration transferability among moisture meter models.

In response to these challenges and with the belief that it was possible to substantially improve the RF dielectric moisture method, two agencies of the US Department of

Agriculture (USDA-Grain Inspection, Packers and Stockyards Administration (GIPSA) and USDA-Agricultural Research Service (ARS)) initiated a collaborative research project in 1995. Kurt C Lawrence and Stuart O Nelson (ARS) developed the calibrated dielectric test cell [1] that was subsequently used by GIPSA to measure the dielectric characteristics of thousands of grain samples.

Analysis of that data and other tests at lower frequencies [2] showed:

- The large dielectric loss peaks and steep slopes and the unusually high dielectric constant values observed in the kilohertz and low megahertz frequency regions are due to conductivity effects—Maxwell–Wagner relaxations and electrode polarization—and not to bound water. These conductivity effects are extremely sensitive to the distribution of moisture within kernels and subtle differences in kernel morphology—contributing significantly to moisture meter calibration instability within grain types and calibration diversity across grain types.

- Moving the measurement frequency for dielectric moisture meters from the 1–20 MHz range to about 150 MHz (specifically, 149 MHz), where dielectric loss appeared to be minimized, dramatically reduces the influence of conductivity effects on moisture measurements and improves calibration accuracy and stability.
- For grain, the Landau–Lifshitz, Looyenga density correction as restated by Nelson [3] effectively normalizes grain samples to a common density—thereby minimizing density-induced errors from test cell loading, grain moisture level, and kernel density and shape.
- After density correction, the shapes of the dielectric constant (at 149 MHz) versus moisture curves for all grain types became geometrically similar and could be superimposed by three ‘unifying parameters’. After the unifying adjustments, all grain types could be described by a single calibration equation.

The water in grain (for dry to moderately moist samples) appears to be ‘bound’ in the sense that it does not freeze at 0 °C, but there seems to be a difference in the dielectric response of ‘tightly-bound’ or ‘monolayer’ water and the dielectric response of the rest of the water in grain.

Based on these insights, GIPSA developed the ‘Unified Grain Moisture Algorithm’ (UGMA). In this method, many similar types of grains (such as wheat classes, rough rice classes, edible beans, processed rice, etc) are grouped together to use exactly the same calibrations. Furthermore, distinctly different types of cereal grains and oilseeds are combined into a single calibration by means of unifying parameters as described below. The accuracy of the method, with a single unified calibration, was shown to be as good as or better than that achievable with current dielectric grain moisture meters using separate calibrations for each distinct grain type [2].

GIPSA decided to publish the UGMA as a public algorithm rather than seeking patent protection and exclusive licensing. GIPSA did this to enable multiple manufacturers to design and produce grain moisture meters that should require little or no calibration development effort and that should yield equivalent moisture measurement results for different meter models. Also, GIPSA has supported research at Corvinus University of Budapest to further refine the algorithm and answer several researchable questions that are of common interest to all participating manufacturers.

This paper provides an overview of the Unified Grain Moisture Algorithm and presents an updated summary of performance data for over 6000 samples representing 53 US grain types and 6 crop years. Methods for transferring grain moisture calibrations from the original ‘Master’ test cell to a smaller test cell were developed and tested. Three temperature correction functions with differing levels of complexity were evaluated.

## 2. Materials and methods

### 2.1. Grain samples

*2.1.1. Samples for calibration development and testing.* Obtaining thousands of grain samples that are representative of diverse growing regions, varieties, moisture levels and

**Table 1.** Grain samples for transferability and temperature correction tests.

Grain group	Transferability test		Temperature test	
	Samples	Moisture range	Samples	Moisture range
Soybeans	75	8–24	6	10–19
Sorghum	12	13–26	–	–
Sunflower	36	5–36	11	5–24
Corn	93	9–44	8	7–22
Oats	6	9–19	8	13–22
Wheat	63	9–24	12	7–29
Barley	24	10–17	6	11–20
Rough rice	91	9–25	–	–
Rapeseed	–	–	8	9–14

crop years is very difficult. Furthermore, determining the ‘true’ moisture contents of those samples by a well-controlled reference method is extremely expensive. This research overcame those limitations by using the same samples and reference analyses as the GIPSA Annual Moisture Survey [4]. This program involves collecting and testing about 1200 grain samples per year that represent all significant growing areas for all US grain crops that are assigned to GIPSA for quality certification. The purpose of the Annual Moisture Survey is to ensure that official moisture meters (used by the US Official Inspection Service) are calibrated to provide the best accuracy possible with respect to the USDA air-oven method. Thus, this RF dielectric research project was a logical and effective extension of the Annual Moisture Survey.

*2.1.2. Samples for calibration transfer tests.* The successful commercialization of the UGMA requires that calibration parameters be transferable among ‘UGMA-compatible’ instrument models. The calibration transfer comparisons involved 400 samples representing 8 grain groups and a total of 15 grain types. These were a subset of 2004-crop samples from the USDA-GIPSA Annual Moisture Survey. The grain groups, number of samples and moisture ranges are listed in table 1. Note that some grain groups included multiple grain types; the wheat group, for instance, included five classes of wheat.

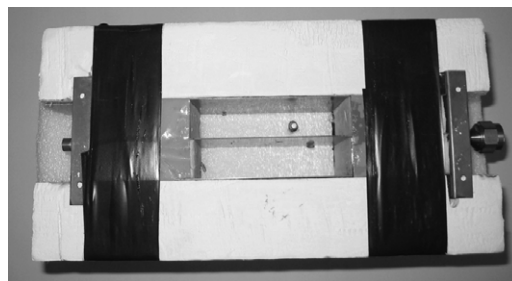
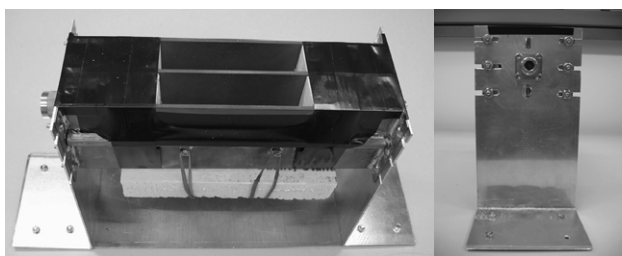
*2.1.3. Samples for temperature correction tests.* The temperature correction tests were performed at Corvinus University of Budapest with grain samples of Hungarian origin. Bulk samples were obtained from grain receiving stations in Hungary (Herceghalom and Szombathely). The grain types tested included: soybeans, soft wheat, sunflower, rapeseed, autumn barley and oats. The moisture content of the samples was adjusted as necessary by adding distilled water to the samples, mixing the samples thoroughly in sealed containers and allowing them to equilibrate under refrigeration for at least 1 week prior to testing. Table 1 lists the number of portions and moisture ranges for each sample type tested.

### 2.2. Apparatus

*2.2.1. Test cells.* Each of the three test cells (figures 1–3) that were used in this research was constructed as a parallel-plate transmission line (three parallel plates). The characteristic

**Table 2.** Test cell dimensions.

Test cell (figure no.)	Plate height (mm)	Air sections length (mm)	Grain section length (mm)	Spacing (mm)	Volume (ml)	Plate thickness (mm)
Master (1)	90.0	223.8	152.4	31.4	861	4.8
Prototype VI (2)	76.2	63.5	101.5	26.8	415	3.2
Temperature (3)	76.2	63.7	101.6	25.4	393	0.8

**Figure 1.** Master transmission-line test cell, loading funnel and HP-4291A RF Material/Impedance Analyser.**Figure 3.** Parallel-plate transmission-line cell for temperature tests, with extruded polystyrene insulating jacket (top removed).**Figure 2.** Prototype VI test cell.

impedance of each test cell was adjusted (by varying the spacing between the plates) to approximately  $50 \Omega$ . The optimum spacing was selected to minimize the magnitude of the reflection coefficient for the empty test cell (over the frequency range of 1 to 250 MHz) when terminated with a precision  $50 \Omega$  load. The grain-filled section for each test cell was centred between two air-filled sections. The purpose of the air-filled sections on either side of the grain-holding section was to avoid effects caused by non-TEM modes that might be excited at the abrupt transitions at either end of the test cell. The grain section was defined by thin polystyrene plates in the 'Master' test cell and by blocks of Owens-Corning Pink<sup>®</sup> extruded polystyrene (dielectric constant, approximately 1.08) for the 'Prototype VI' and 'Temperature' test cells. Lawrence *et al* [1] provide more mechanical details of the Master test cell design. The general dimensions for the three test cells are given in table 2.

Figure 2 shows two views of the Prototype VI test cell that was used to test calibration transferability. This test cell was dimensioned to be more practical for commercial implementation than the Master test cell. The air-filled and grain-filled sections were both shortened substantially. The height of the test cell plates was reduced, and the spacing of the plates was reduced proportionately to maintain  $50 \Omega$  characteristic impedance. The parallel plates were made from 3.2 mm double-sided copper-clad epoxy-glass circuit board material. This material was chosen because it offered

mechanical rigidity and ease of fabrication and mounting for the centre plate.

At each end of the centre plate, the copper cladding (both sides) was removed from a 6 mm wide vertical strip to provide an insulating gap similar to the air gap on the Master test cell. Two 10 mm tabs were machined on each end of the centre plate to fit tightly in matching slots in the endplates of the test cell. (See the test cell end-view in figure 2.) At each end of the test cell, N-type panel connectors were fastened with screws to the endplates, and the centre contacts were connected to both sides of the centre plate through 6 mm sections of 4 mm diameter brass tubing. A piece of 25 mm thick extruded polystyrene foam was used for the removable gate beneath the grain-filled section. The test cell was mounted on aluminium end supports that were bolted to an aluminium plate (approx.  $102 \text{ mm} \times 330 \text{ mm} \times 0.76 \text{ mm}$  thick).

The same precision  $50 \Omega$  load (HP-909C) was used to terminate the Master and Prototype VI test cells during grain tests.

Figure 3 shows the test cell that was used for temperature correction tests. Its design was similar to that of Prototype VI except the outer plates were made of thin solid copper and the inner electrode was made of thin double-sided copper-clad circuit board material. At each end of the centre plate, a 1 cm wide strip of copper cladding (both sides) was removed except for where the copper was soldered to a SMA-type coaxial connector. Pieces of rigid extruded polystyrene foam insulation (Owens-Corning PINK<sup>®</sup>,  $\epsilon_r$  approx 1.08) were used as spacers between the plates, to define the grain-filled section, and to provide an insulating jacket that completely surrounded the test cell during temperature tests. The test cell was terminated with a precision SMA-type 50-ohm load.

**2.2.2. Instrumentation.** A Hewlett-Packard HP-4291A RF Material/Impedance Analyser<sup>3</sup> was used to record complex reflection coefficient data (at 2 MHz intervals from 1 to

<sup>3</sup> Mention of products or trade names does not imply recommendation or endorsement by USDA over other similar products not mentioned.

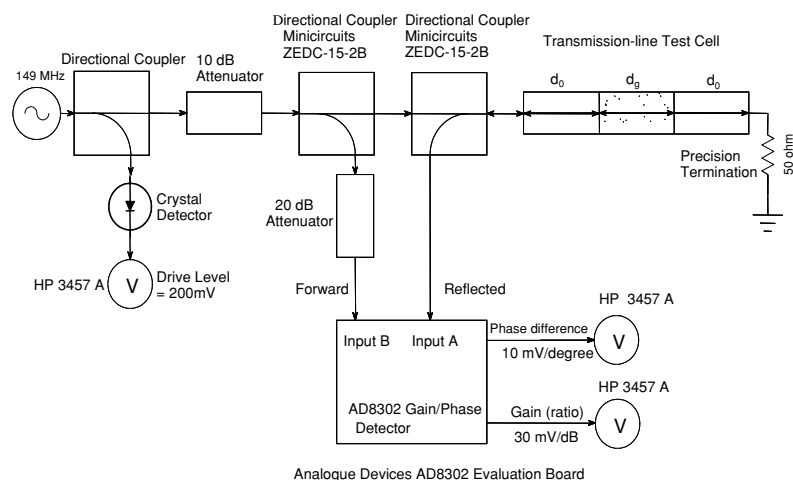


Figure 4. VHF prototype sensor block diagram.

501 MHz) for the calibration data collection and the calibration transferability tests.

The simplified single-frequency reflectometer system shown in figure 4 was used to measure dielectric characteristics at 149 MHz for the temperature correction tests. The 149 MHz signal source was a G4-107 VHF signal generator. The signal generator output amplitude was monitored with a 10 dB directional coupler and a diode detector. An Analog Devices AD-8302 Gain/Phase Detector (evaluation board) provided an output that was proportional to the logarithm of the ratios of the reflected and incident signal magnitudes at the test cell and an output that was proportional to the phase difference between the incident and reflected signals. An Analog Devices AD-590 temperature sensor (1  $\mu$ A per K) was immersed in the grain in the test cell.

The dc voltages from the level detector and the gain/phase detector and the current from the AD-590 temperature sensor were measured by an HP-3457A digital multimeter, which was controlled by a PC-compatible computer through a GPIB card. The software checked the temperature every 30 s and recorded a set of readings each time the sample temperature had changed by more than 0.5  $^{\circ}$ C from the temperature of the previously recorded data. This permitted unattended operation during the lengthy sample equilibration periods.

The gain  $V_G$  and phase  $V_P$  signals from the AD-8302 detector system were converted to complex reflection coefficient  $\Gamma$  as in (1). Equation (1) was derived from the AD-8302 data sheet and gain-phase comparison tests with the HP-4291A Material/Impedance Analyser. The gain voltage with the reflectometer output shorted ( $\Gamma = -1$ ) was 1.45 V. The phase sensitivity of the reflectometer was 87.609 degrees per volt, and the gain sensitivity was 0.60 V per decade of voltage ratio change.

$$\Gamma = \left[ 10^{\left( \frac{V_G - 1.45}{0.6} \right)} \cdot \exp(i \cdot (51.033 + 87.609 \cdot V_P)) \right]. \quad (1)$$

### 2.3. Test methods

**2.3.1. Calibration development and evaluation.** Before each day's tests, the HP-4291A system was calibrated according to the manufacturer's recommendations by means of tests with

open, short and 50  $\Omega$  terminations [5]. The reference plane was established at the N-type connector on the source end of the test cell. Immediately prior to loading each sample into the loading funnel, the temperature of the sample was determined with a thermocouple-type digital thermometer (0.1  $^{\circ}$ C resolution). Samples were loaded into the test cell through a funnel (Seedburo Model 151) whose outlet was positioned 50 mm over the centre of the grain-filled section. After the sample overflowed the test cell, the excess grain was removed by striking off the grain with a wooden straightedge of the type used for US official test weight (bulk density) measurements. A zigzag motion was imparted to the straightedge to achieve consistent filling of the test cell. The excess was removed from the vicinity of the test cell before initiating the complex reflection coefficient measurement (a reading every 2 MHz from 1 to 501 MHz). After the reflection coefficient measurements, the sample was emptied from the test cell and weighed (0.1 g resolution). The actual moisture content of each sample was determined by the applicable official USDA air-oven method [6].

**2.3.2. Calibration transferability evaluation.** The tests that were performed for the calibration transferability evaluation were executed the same as described in section 2.3.1 except that each day, tests were performed for all available samples first with the Master test cell and afterwards with the Prototype VI test cell.

**2.3.3. Temperature correction evaluation.** Grain was poured slowly into the test cell while the test cell was shaken to settle the sample. After loading, the top of the test cell was sealed with wide plastic adhesive tape to minimize moisture loss. The test cell was placed in a laboratory freezer (approx.  $-25^{\circ}$ C) and allowed to equilibrate for at least 12 h. Then, the insulated test cell assembly was removed from the freezer, covered with a piece of polystyrene foam insulation, transported to the laboratory area (approx.  $22^{\circ}$ C), connected to the measuring system, and allowed to warm to room temperature (for about 8 h). When the grain had warmed to near room temperature, the automatic data collection sequence was manually terminated. After that, the uncovered test cell was

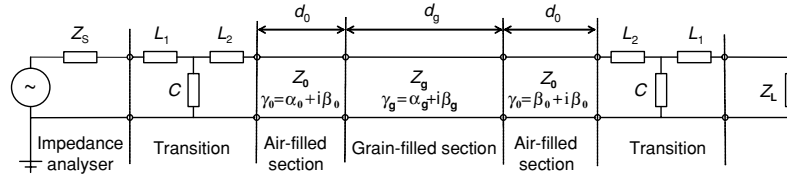


**Figure 5.** Block diagram of the ABCD matrix model.

placed in a laboratory oven (approx. 50 °C) and allowed to equilibrate for at least 6 h. Then the test cell was removed from the oven, covered and reconnected to the measuring system. When the grain had cooled to near room temperature (after about 10 h), the automatic data collection sequence was again terminated. The grain was emptied from the test cell and weighed so that the sample density could be determined. The reference moisture value for each test sample was determined by the appropriate Hungarian Ministry of Agriculture standard air-oven method (Hungarian Standard 6367/3-83).

#### 2.4. Data analysis methods

The data (sample number, air-oven moisture, sample mass, temperature and complex reflection coefficient) were collected into separate files by grain type for processing. The reflection coefficient data were converted to effective dielectric constant by means of two types of models (for comparison). All mathematical algorithms were coded with Mathcad Version 2001i [7].

**2.4.1. Signal flow graph model.** The signal flow graph model of the test cells described two transmission-line sections and two interfaces: the air-filled section nearest the signal source, the interface between the first air-filled section and the grain filled section; the grain-filled section, and the interface between the grain filled section and the second air-filled section nearest the precision 50  $\Omega$  termination. Because the characteristic impedance of the transmission-line test cell was assumed to be 50  $\Omega$ —matched to the termination—the length of the second air-filled section did not appear in the resulting mathematical model (2):

$$\Gamma_m = \exp(-2 \cdot i \cdot \omega \cdot d_0 \cdot \sqrt{\epsilon} \cdot c^{-1}) \cdot \frac{1 - \sqrt{\epsilon}}{1 + \sqrt{\epsilon}} \times \frac{1 - \exp(-2 \cdot i \cdot \omega \cdot d_g \cdot \sqrt{\epsilon} \cdot c^{-1})}{1 - \exp(-2 \cdot i \cdot \omega \cdot d_g \cdot \sqrt{\epsilon} \cdot c^{-1}) \cdot \left(\frac{1 - \sqrt{\epsilon}}{1 + \sqrt{\epsilon}}\right)^2} \quad (2)$$

where  $\Gamma_m$  is the measured reflection coefficient,  $\omega$  is the angular frequency in radians,  $d_0$  is the air-filled section length,  $d_g$  is the grain-filled section length,  $c$  is the velocity of light and  $\epsilon$  is the bulk grain effective complex permittivity.

Kurt C Lawrence, who performed the original modelling, adjustment and calibration of the test cell, provided measurements of several types of alcohols. The test cell parameters for the signal flow graph model were determined by optimizing the agreement between the predicted complex permittivity (from complex reflection coefficient) and the known dielectric characteristics of the high-purity alcohols [2].

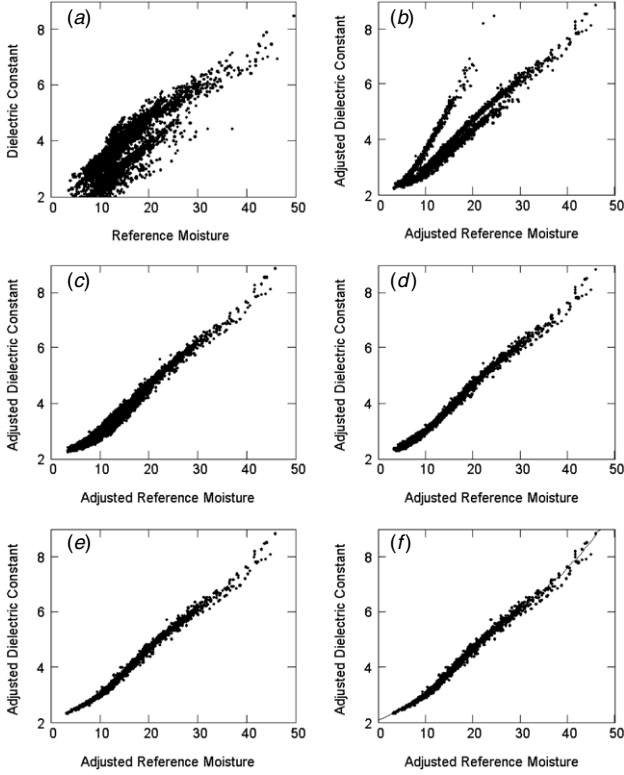
**2.4.2. ABCD matrix model.** More flexible models were created based on the ABCD matrix approach. Briefly, the ABCD matrix approach involves describing a complex 2-port device as a series of simpler 2-port devices that can each be explicitly modelled as  $2 \times 2$  complex (ABCD) matrices. Matrix multiplication of the series of matrices yields a single ABCD matrix that can be converted to scattering ( $S$ ) parameters and (for a defined load impedance) to complex reflection coefficient of the system as seen at the input port. Mongia *et al* [8] provide an accessible explanation of the ABCD matrix method.

Figure 5 shows the block diagram of the elements that were included in the ABCD matrix model. Each of the transmission-line sections was defined by its length, characteristic impedance ( $Z$ ) and complex propagation constant ( $\gamma$ ). Furthermore, the transitions at either end of the test cell were modelled as lumped parameters ( $L_1$ ,  $L_2$  and  $C$ ) and the source and termination impedances ( $Z_S$  and  $Z_L$ ) could be varied from the nominal value of 50  $\Omega$ . Space limitations preclude showing the details of the ABCD matrix model; it is available upon request from the authors as a ‘live’ Mathcad document.

The signal flow graph model and the ABCD matrix model both yield complex reflection coefficient values from complex permittivity values, but the calculation that was needed was to go the other direction—from complex reflection coefficient to complex permittivity. An iterative nonlinear solver (based on the Mathcad *FIND* function) was used with both model types to determine the complex (effective) permittivity from the measured complex reflection coefficient. The extra modelling flexibility afforded by the ABCD matrix approach was not needed to characterize the Master test cell; the simpler signal flow graph model yielded equivalent results for well-matched test cells.

**2.4.3. Additional model corrections.** Other research [9] has shown that the dielectric constant data needed to be corrected for two effects that were caused by the test cell design. The presence of dielectric materials in proximity to the test cell (specifically the cell ‘gate’) caused the calculated dielectric constant of the empty test cell to be other than 1.000. To correct this, the empty-cell dielectric constant  $\epsilon_{ec}$  (calculated from the empty-cell reflection coefficient) and an offset value *corr* were subtracted from the measured relative complex permittivity  $\epsilon_m$  for the sample as in (3).

Secondly, the parallel-plate transmission-line test cell did not support a true transverse-electric-magnetic (TEM) mode with grain in the test cell. That is, a portion of the electromagnetic wave propagated outside the region between the parallel plates. An effective filling fraction  $q$  [8] was needed to convert the measured (or effective) relative complex



**Figure 6.** Visualizing the Unified Grain Moisture Algorithm. (a) Dielectric constant versus reference moisture for 6189 samples representing 53 types of US cereal grains, oilseeds, pulses and processed rice for 1998 through 2003 crop years. (b) With density correction and reverse temperature correction (of reference moisture values). (c) With slope ( $P_S$ ) adjustment. (d) With offset ( $P_O$ ) adjustment. (e) With translation ( $P_T$ ) adjustment. (f) With best-fit fifth-order polynomial calibration curve superimposed on the data.

permittivity to ‘actual’ relative complex permittivity. The real part  $\varepsilon_r$  of the relative complex permittivity was used for further calculations. For the Master test cell, the nominal value of  $\varepsilon_{cc} + corr$  was 1.18, and the optimum value for  $q$  was 0.752.

$$\varepsilon_r = \text{Re}(\varepsilon_m - \varepsilon_{cc} - corr) \cdot q^{-1} + 1. \quad (3)$$

Figure 6(a) shows calculated  $\varepsilon_r$  versus reference moisture values for 6189 samples that represented 53 different grain types and 6 crop years.

**2.4.4. Density correction.** Funk [2] showed that the density-corrected dielectric constant is much more useful for grain moisture prediction than the uncorrected dielectric constant. The Landau and Lifshitz, Looyenga dielectric mixture equation as restated by Nelson [3] was found to be particularly effective for adjusting the dielectric constants of different grain samples to a common density (target density). This correction minimizes errors and nonlinearity caused by three major sources of density variations: moisture level, filling method and sample-to-sample variation. Density correction in the UGMA was performed as in (4).

$$\varepsilon_c = \left[ (\varepsilon_r^{1/3} - 1) \cdot \frac{\rho_t}{\rho_s} + 1 \right]^3 \quad (4)$$

where  $\varepsilon_c$  is the density-corrected dielectric constant,  $\varepsilon_r$  is the dielectric constant,  $\rho_t$  is the target density ( $67.4 \text{ kg hl}^{-1}$ ),  $\rho_s$  is the sample density ( $\text{kg hl}^{-1}$ ).

A target density of  $67.4 \text{ kg hl}^{-1}$  was chosen because it was the average density of the samples tested. The choice of target density was arbitrary; trials with different values showed that the specific value did not affect the accuracy of the resulting calibrations. However, the target density determined the slope of the relationship between density-corrected dielectric constant and moisture, and it affected the specific polynomial calibration coefficients that were found by regression. Figure 6(b) shows the density-corrected dielectric constant versus air-oven moisture values (reverse temperature corrected as in (5)) for the same 6189 grain samples. A reduction in scatter and improved linearity (within groups) is evident.

**2.4.5. Unifying adjustments.** After density correction, the loci of data points (plotted as dielectric constant versus adjusted air-oven moisture) for all grain groups were geometrically similar; the data for different grain groups were superimposed by applying the unifying parameters defined in equations (5)–(7). Note that ‘reverse’ (positive) temperature correction was applied to the air-oven moisture values (5) to simplify the curve-fitting process. For each grain group, the slope (% moisture per unit of density-corrected dielectric constant) was calculated for the subset of samples with reference moisture values between 10 and 20% moisture. (Grain types were initially assigned to groups based on similarities in chemical and physical characteristics. Group memberships were later adjusted as needed to minimize calibration error.) The samples below 10% moisture and above 20% moisture were excluded from the slope calculation because the ‘standard’ curve shape is less linear in those regions.

The slope unifying parameter  $P_S$  (6) was defined as the correction factor needed to adjust the slope of each grain group to 6.000 in the 10–20% moisture range. (Note that the y-axis in figure 6 represents the independent variable.) The data for the different grain groups appeared to rotate about a point ( $\%M = 5$ ,  $\varepsilon_c = 2.5$ ), so an offset unifying parameter  $P_O$  with a nominal value of 2.5 was hypothesized. Figure 6(c) shows the data for the 6189 samples with the slope unifying parameter  $P_S$  applied; data curves for all grain groups are now parallel in the 10–20% moisture range.

The offset unifying parameter  $P_O$  was iteratively adjusted for each grain group, resulting in figure 6(d). A translation unifying parameter  $P_T$  was needed to align the curve shapes for the different grain groups in the low-moisture region. Note that changing the translation parameter had the effect of translating the data for that grain group along the common (slope = 6.000) line. After applying the three unifying parameters to each grain group, the data appeared as in figure 6(e). Current estimates of unifying parameters for some of the most important grain groups are shown in table 3. A fifth-order polynomial was fitted to the  $\varepsilon_{adj}$  and  $M_{adj}$  data as shown in figure 6(f). The current polynomial coefficient  $C$  estimates are given in table 4. Predicting moisture values  $M_{pred}$  as in (7) required ‘backing out’ the translation parameter  $P_T$ .

$$M_{adj} = M_{ref} + K_t \cdot (T - 25) + P_T \quad (5)$$

**Table 3.** Unifying parameters and temperature correction coefficients for selected grain groups.

Grain group	$P_O$	$P_S$	$P_T$	$K_T$
Soybeans	2.113	0.80	-1.00	0.107
Sorghum	2.455	1.10	0.50	0.108
Sunflower	2.720	0.54	1.50	0.054
Corn	2.547	1.00	0.00	0.093
Oats	2.395	1.07	0.50	0.143
Wheat	2.388	1.15	0.30	0.088
Barley	2.287	1.07	-1.00	0.113
Rice	2.424	1.12	0.50	0.077
Rapeseed	2.430	0.80	0.00	0.081

**Table 4.** Polynomial calibration coefficients for predicting moisture content from adjusted dielectric constant as in (7).

$C_0$	$C_1$	$C_2$	$C_3$	$C_4$	$C_5$
-92.3409	88.472	-30.686	5.4197	-0.45341	0.014437

$$\varepsilon_{\text{adj}} = (\varepsilon_c - P_O) \cdot P_S + 2.5 + \frac{P_T}{6} \quad (6)$$

$$M_{\text{pred}} = \left( \sum_{r=0}^5 (\varepsilon_{\text{adj}})^r \cdot C_r \right) - P_T. \quad (7)$$

**2.4.6. Temperature correction.** Temperature significantly influences the radio-frequency dielectric characteristics of grain; the dielectric constant generally increases with increasing temperature. Previous research [2] suggested a simple temperature correction function (8) for reducing temperature-induced error in UGMA predicted moisture values.

$$M_{\text{tc}} = M_{\text{pred}} - K_T \cdot (T - 25) \quad (8)$$

where  $M_{\text{pred}}$  is the moisture value calculated from dielectric characteristics,  $K_T$  is the temperature correction coefficient (% moisture per degree Celsius),  $T$  is the measured sample temperature,  $M_{\text{tc}}$  is the predicted moisture content with temperature correction.

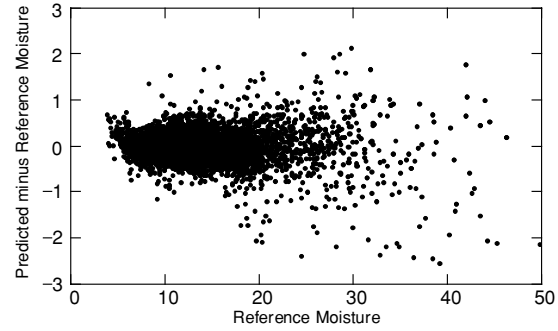
Two additional temperature correction functions were evaluated. Equation (9) was linear with sample temperature and linearly dependent on sample (predicted) moisture. Equation (10) added a term that was quadratic in temperature. Note that to apply (9) and (10),  $M_{\text{pred}}$  is used for  $M_{\text{pred}'}$  initially and the calculated value of  $M_{\text{tc}}$  is iteratively substituted for  $M_{\text{pred}'}$  until  $M_{\text{tc}}$  converges. Alternatively, (11) and (12) (found by setting  $M_{\text{pred}'}$  equal to  $M_{\text{tc}}$ ) can be used in place of (9) and (10), respectively, without iteration.

$$M_{\text{tc}} = M_{\text{pred}} - (K_{\text{to}} + K_{\text{ts}} \cdot M_{\text{pred}'}) \cdot (T - 25) \quad (9)$$

$$M_{\text{tc}} = M_{\text{pred}} - (K_{\text{to}1} + K_{\text{ts}1} \cdot M_{\text{pred}'}) \cdot (T - 25) - K_{\text{tq}1} \cdot (T - 25)^2 \quad (10)$$

$$M_{\text{tc}} = \frac{M_{\text{pred}} - K_{\text{to}} \cdot (T - 25)}{1 + K_{\text{ts}} \cdot (T - 25)} \quad (11)$$

$$M_{\text{tc}} = \frac{M_{\text{pred}} - K_{\text{to}1} \cdot (T - 25) - K_{\text{tq}1} \cdot (T - 25)^2}{1 + K_{\text{ts}1} \cdot (T - 25)}. \quad (12)$$

**Figure 7.** Moisture prediction error for 6189 grain samples representing 53 US grain types and 6 crop years.

### 3. Results and discussion

#### 3.1. Accuracy of the Unified Grain Moisture Algorithm

Figure 7 and table 5 present the performance of the UGMA for the 6189 samples tested in 1998 through 2003. (The original UGMA publication [2] included only data for 1998 through 2000.) The overall prediction accuracy (standard deviation of error with respect to the air-oven method) was 0.34% moisture. The error increased somewhat for high moisture grain; the grain groups that had very wide moisture ranges tended to have poorer overall prediction accuracy.

#### 3.2. Calibration transfer accuracy

Two mathematical approaches (grain-independent and grain-specific) were used to transfer calibrations (unifying parameter and polynomial regression coefficients) from the original Master test cell to the smaller Prototype VI test cell.

**3.2.1. Grain-independent standardization.** Wheat (63 samples representing 5 classes of wheat) was chosen as the ‘transfer’ standard for the grain-independent standardization. The test cell signal-flow-graph model parameters for the Prototype VI cell (air-filled length, empty cell correction factor and effective filling fraction) were adjusted to achieve minimum differences between the density-corrected dielectric constant values (and, therefore, the predicted moisture values) for wheat for the Master and Prototype VI test cells. The existing unifying parameters and polynomial regression coefficients (those developed based on 1998 to 2003 data) were used to predict moisture content for 400 samples of 8 grain groups (15 types).

Figure 8(a) shows the moisture prediction errors (with respect to the air-oven moisture values) for the Master test cell for all grain groups. Figure 8(b) shows the prediction errors for the Prototype VI test cell. (The wheat data are indicated by filled circles in figures 8(b) and (d).) Figure 8(d) shows the standardization errors (predicted moisture for the Prototype VI test cell minus the predicted moisture for the Master test cell).

The solid ‘funnel’ lines in figures 8(a)–(c) represent the moisture accuracy tolerances (with respect to the air-oven method) for corn, rice, oats and sunflower that have been established by the US National Conference on Weights and Measures (NCWM) [11]. The lines in figures 8(d) and (e)

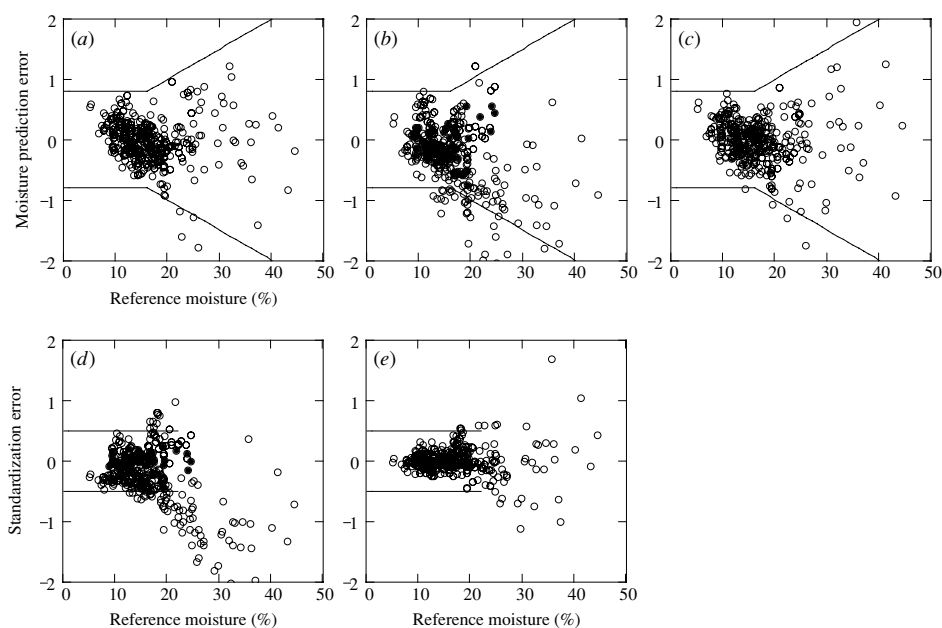


**Figure 8.** Moisture prediction errors with respect to the air-oven method for the Master test cell (a), for Prototype VI test cell with grain-independent standardization (b) and for Prototype VI test cell with grain-specific standardization (c). Standardization errors (differences between Prototype VI and Master test cells) for grain-independent standardization (d) and grain-specific standardization (e).

**Table 5.** Grain samples and moisture ranges tested during 1998 through 2003 by grain group, with accuracy stated as standard error of prediction (SEP).

Grain group name	Types in group	Number of samples	Moisture range (%M)	Accuracy SEP (%M)
Soy	1	795	6–26	0.18
Sorghum	1	216	5–25	0.22
Sunflower seed	2	564	4–25	0.38
Corn	3	1234	4–50	0.47
Oats	1	136	4–16	0.32
Wheat (except Durum)	5	1232	7–26	0.22
Barley	2	383	5–21	0.28
Rough rice and Durum	4	862	4–37	0.43
Peas	3	90	7–20	0.24
Mustard	2	39	5–13	0.29
Edible beans group 1	9	147	7–22	0.38
Edible beans group 2	2	30	9–17	0.41
Processed rice	11	304	11–20	0.28
Long-grain proc. rice	2	56	11–21	0.23
Triticale	1	12	10–14	0.17
Canola and rapeseed	2	16	4–8	0.29
Safflower	1	12	4–10	0.41
Flaxseed	1	28	5–11	0.12
High-oil corn	1	33	9–29	0.18
Total	53	6189	4–50	0.34

are the tolerances ( $\pm 0.5\%$  moisture up to 22% moisture) established by NCWM for meter-to-meter comparison tests.

With the simple standardization based on wheat as described above, the agreement between the two test cells was reasonably good for all grain groups in the low moisture range (below about 20% moisture), but the agreement was progressively poorer at higher moisture. Corn and sunflower seed, which had the widest moisture ranges, were most affected. Figure 9 presents the results for each grain group individually. Mean differences are marked by circles and the error bars represent plus and minus one standard deviation

of the differences. Figure 9(d) shows small but potentially significant mean differences between the two test cells for different grain groups. Also, residual plots for individual grain groups showed significant slope differences—especially between rice and sunflower seed.

Manual adjustments and an automated solver (written in Mathcad programming language) were used to seek test cell model parameters (for the signal-flow-graph model and the ABCD matrix model) that would eliminate the slope differences and mean differences among grain groups. No grain-independent approach was entirely successful. For



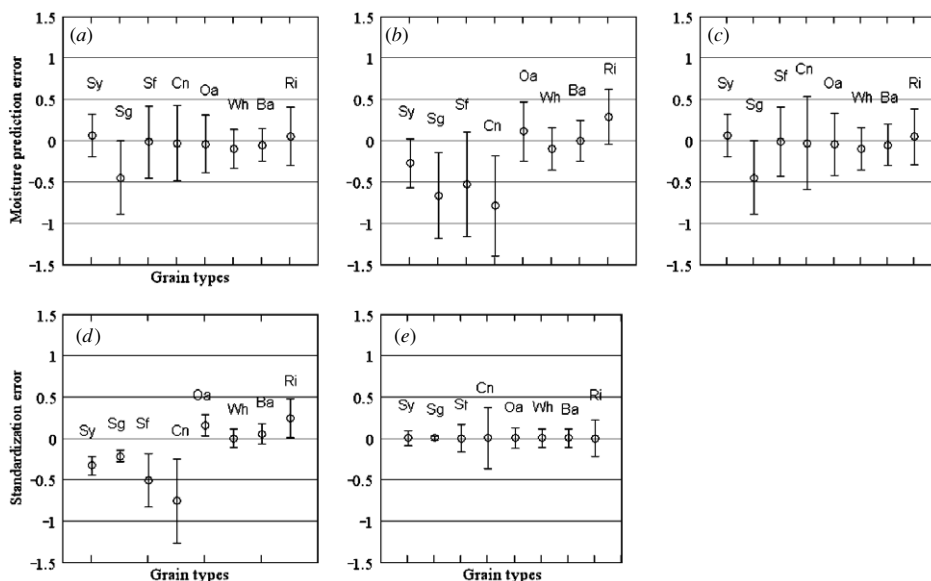


**Figure 9.** Moisture prediction errors (mean, and plus and minus one standard deviation) for seven grain groups. Errors with respect to air-oven are shown: (a) for Master test cell, (b) for Prototype VI test cell with grain-independent standardization and (c) for Prototype VI test cell with grain-specific standardization. Standardization errors (differences between Prototype VI and Master test cell results) are shown: (d) for grain-independent standardization, and (e) for grain-specific standardization. Sy: soybeans, Sg: sorghum, Sf: sunflower seed, Cn: corn, Oa: oats, Wh: wheat, Ba: barley and Ri: rice.

example, adjusting the assumed characteristic impedance of the transmission line in the model was capable of minimizing the differences between rice and sunflower seed—but at the expense of greater differences for corn. This suggested that the differences between test cell responses for different grain types were not due to differences in the electrical characteristics of the test cells, but rather due to differences in the size and shape of the test cells (relative to kernel dimensions) or some other effect that would respond differently to different grain types. The differences among grain types did not appear to be correlated to grain bulk density.

Other UGMA research [12] revealed significant differences in dielectric response for different test cell loading methods. Those differences appeared to be due to systematic differences in kernel orientation—especially for elongated kernels such as oats and barley. Slight systematic orientation differences (in spite of similar loading methods for both test cells) may have been responsible for the differences in dielectric response observed in this research; however, further research is needed to confirm that hypothesis.

**3.2.2. Grain-specific standardization.** A second level of standardization (beyond the wheat-only standardization described above) was applied to minimize the differences among grain groups. The slope and offset unifying parameters ( $P_S$  and  $P_O$ ) for each grain group were adjusted slightly to eliminate the mean differences and slope differences among grain groups. Figures 8(c), (e), 9(c) and (e) show the moisture accuracy and standardization agreement that were achieved after grain-specific standardization.

Figures 9(a), (b) and (d) show that the standard deviations of differences between results for the two test cells (with only the simple standardization) are small relative to the standard deviations of the errors with respect to the air-oven moisture values for either test cell (except for corn and sunflower

seed where slope differences inflated the values). Therefore, the intent of achieving close agreement among instruments appears to be achievable, though some adjustments in the unifying parameters may be needed to align results for different moisture meter models with very different test cells. Figures 9(a) and (c) show that accuracy (with respect to the air-oven moisture) of the Prototype VI test cell after grain-specific standardization was essentially equivalent to that of the Master test cell.

### 3.3. Temperature correction

Accurate moisture measurement over a wide temperature range is a critical requirement for grain moisture meters [11]. Therefore, optimizing the temperature correction functional form and specific coefficients was considered very important to the success of the Unified Grain Moisture Algorithm.

Figure 10 shows typical results for one of the grain types that were tested (wheat). Each ‘curve’ is the set of data points for a sample portion at one moisture level. For some samples, only the low temperature part of the test was performed. Curves are labelled with the corresponding air-oven moisture values. Figure 10(a) presents the predicted moisture values without temperature correction. Without temperature correction, the predicted values increased with increasing temperature for all samples. The wheat samples at moisture levels above 20% showed slope discontinuities at zero Celsius. The slope discontinuities became more prominent at higher moisture levels. Those discontinuities are believed to be due to the phase change of the ‘free’ water in the samples. The average slope (% moisture per degree Celsius) for the 0–50 °C temperature range was calculated for each sample. The average slope for all samples (of the grain type) was used as the  $K_t$  value in the correction defined in (8). Figure 10(b) shows the effects of that simplest temperature

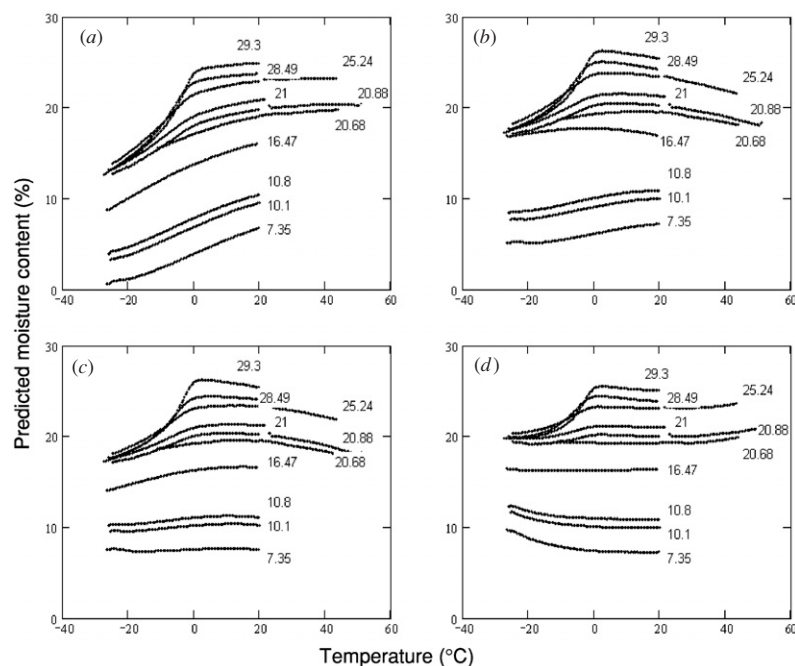


**Figure 10.** Predicted moisture values for wheat samples at 149 MHz with four different temperature correction methods: (a) no temperature correction; (b) constant temperature correction (8); (c) linear moisture-dependent temperature correction (9); (d) linear moisture-dependent temperature correction with quadratic temperature term (10).

correction approach. The average slope (for all samples taken together) for temperatures above zero Celsius was forced to zero, but individual samples exhibited significant residual slope errors.

Linear regression was used to determine the optimum  $K_{t0}$  and  $K_{ts}$  coefficients (for each grain type tested) for equation (9). Applying those coefficients in (9) to the predicted moisture data gave the results that are shown in figure 10(c) for wheat. The slopes of the curves for all the samples were near zero in the 0–20 °C temperature range, but some curvature was evident at temperature extremes.

Coefficients for equation (10) were calculated by polynomial regression for each sample. The quadratic temperature term in (10) reduced the error at temperature extremes, as shown (for wheat) in figure 10(d). With the temperature correction provided by (10), the predicted moisture errors (relative to predicted moisture content at 25 °C) were less than 0.6% moisture for all grain samples at temperatures above 0 °C. The usable temperature range extended to –20 °C or lower for samples with moisture levels below the ‘free’ water limit (approx. 20% moisture for wheat).

The coefficients  $K_{tq1}$  of the quadratic term (calculated separately for each sample) were not highly correlated with sample moisture content, so an average value was selected for each grain type. Using only a constant, moisture-independent  $K_{tq1}$  for each grain group avoided a major increase in model complexity. The current estimates of temperature correction coefficients for (8), (9) and (10) are given in table 6.

The negative  $K_{ts}$  values in table 6 show that there was a general decreasing relationship between the linear temperature corrections (per cent moisture per degree Celsius) needed and the sample moisture content. That is, predicted moisture values for higher moisture samples varied less with sample temperature than predicted values for lower moisture samples.

**Table 6.** Temperature correction coefficients for three temperature correction equations (8), (9) and (10) for seven grain types.

Grain type	$K_t$	$K_{t0}$	$K_{ts}$	$K_{t01}$	$K_{ts1}$	$K_{tq1}$
Wheat	0.088	0.159	–0.0051	0.1201	–0.0044	–0.0021
Barley	0.113	0.159	–0.0035	0.1774	–0.0050	–0.0014
Soybeans	0.107	0.226	–0.0099	0.1366	–0.0072	–0.0022
Corn	0.093	0.199	–0.0071	0.1969	–0.0075	–0.0012
Sunflower	0.054	0.092	–0.0028	0.0868	–0.0026	–0.0004
Oats	0.143	0.155	–0.0014	0.1844	–0.0051	–0.0014
Rapeseed	0.081	0.134	–0.0058	0.1745	–0.0098	–0.0013

It cannot be determined from the available data whether that trend continues for extremely low moisture and extremely high moisture samples.

The measure of success of a temperature correction function is how closely the corrected moisture values at other temperatures compare to the predicted moisture values at the reference temperature (typically 25 °C). One way of quantifying that agreement is to calculate the residual slope (after temperature correction) of moisture predictions with respect to temperature. Figure 11 presents the residual slope values for each of the tested samples for each of seven grain types for temperature corrections based on (8), (9) and (10). Zero residual slope was the goal. The residual slopes that are shown were calculated for sample temperatures between 0 and 40 °C. Note the two different sizes of symbols; smaller symbols indicate tests that included only the low (0–22 °C) temperature range.

Figure 11 shows that, in general, the residual slope values were closer to zero for the moisture-dependent corrections than for the moisture-independent corrections. The advantage provided by the extra quadratic temperature term in (10) is not as apparent in figure 11 as in figure 10(d) because the

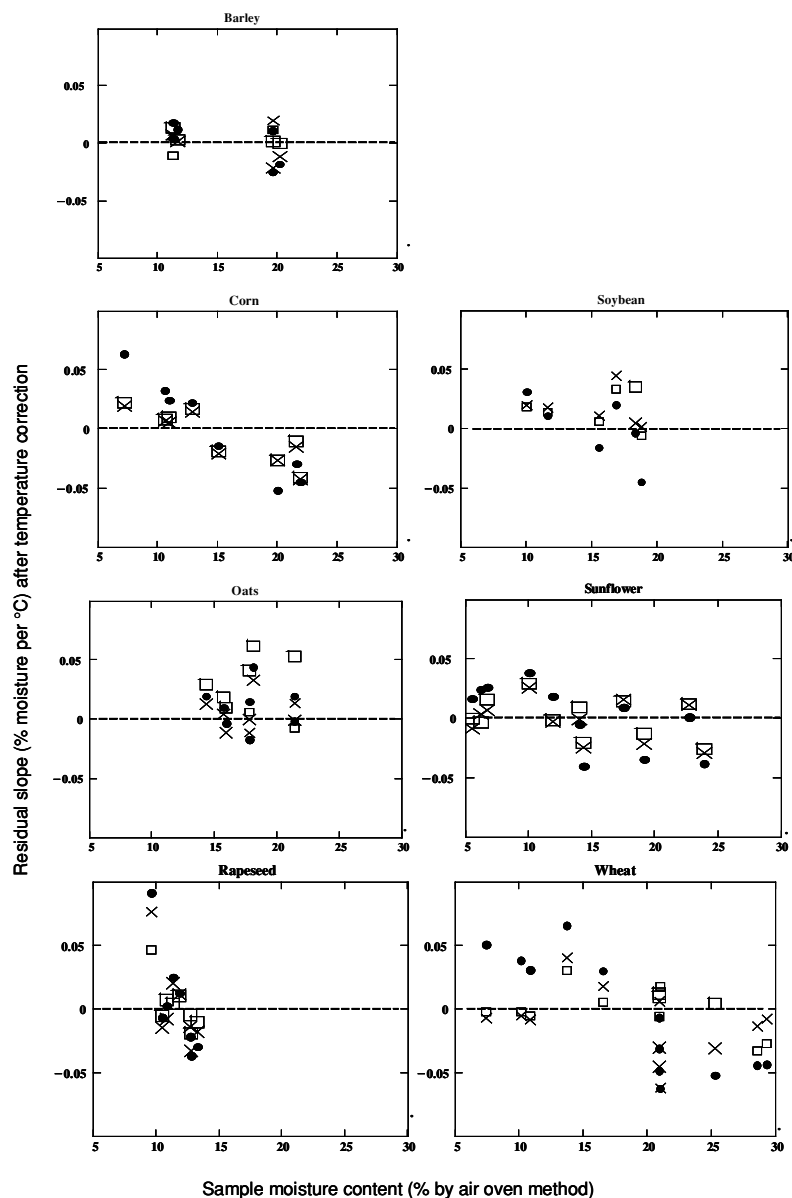


**Figure 11.** Residual (uncorrected) slope of the predicted moisture curve (from 0 to + 40 °C) versus air-oven moisture content for seven grain types. (●) Constant temperature correction as in (8). (×) Linear moisture-dependent temperature correction as in (9). (□) Linear moisture-dependent temperature correction plus a quadratic temperature term as in (10).

temperature range for the slope values in figure 11 did not extend below zero Celsius.

#### 4. Conclusion

The Unified Grain Moisture Algorithm was shown to be applicable to many different grain types and provided good accuracy over wide moisture ranges. Research at Corvinus University of Budapest has improved the method and has made it more suitable for commercialization.

The predicted moisture values for the two test cells tracked closely (as shown by the low standard deviations of differences) with grain-independent or grain-specific standardization. A simple standardization based on one grain type did not completely eliminate offset and slope errors

between the two test cells for all grain types. For high accuracy applications, additional grain-specific standardization may be required. The same basic polynomial regression equation yielded equivalent accuracy for both test cells after grain-specific standardization. With grain-specific standardization adjustments, the differences between results for the two test cells were very small compared to the differences from the air oven.

Three temperature correction functions were evaluated for use with the 149 MHz Unified Grain Moisture Algorithm. Optimum temperature correction coefficients were tabulated for seven grain types. Linear and quadratic moisture-dependent temperature correction functions were found to be more effective than a simple moisture-independent function—especially below 0 °C. More temperature measurements are needed at low moisture levels and high moisture levels

to confirm that a linear moisture-dependent and quadratic temperature-dependent correction is the optimum temperature correction function and to establish the correction coefficients more precisely. Similar tests are needed to determine correction coefficients for additional grain types.

### Acknowledgments

Kurt C Lawrence and Stuart O Nelson, USDA-ARS, Athens, GA, developed and calibrated the original test cell used to collect the dielectric data and loaned a second identical test cell to Corvinus University of Budapest to permit comparison tests. James Rampton, Patricia Jackson, Steven Burton, Lucille Clark, Brenda Evans, Glenn Terrill, and Larry Freese, USDA-GIPSA, performed most of the grain measurements and organized the data. The research regarding the Unified Grain Moisture Algorithm at Corvinus University of Budapest was supported in part by grants and equipment loans and donations from USDA-GIPSA. Viktor Jagasits wrote the QBasic program that was used to control the VHF prototype system to collect the temperature test data.

### References

- [1] Lawrence K C , Funk D B and Windham W R 1999 Parallel-plate moisture sensor for yellow-dent field corn *Trans. ASAE* **42** 1353–7
- [2] Funk D B 2001 An investigation of the nature of the radio-frequency dielectric response in cereal grains and oilseeds with engineering implications for grain moisture meters *PhD Dissertation* University of Missouri–Kansas City
- [3] Nelson S O 1992 Correlating dielectric properties of solids and particulate samples through mixture relationships *Trans. ASAE* **35** 625–9
- [4] GIPSA 1999 Chapter 2—moisture meter calibration *Moisture Handbook* <http://archive.gipsa.usda.gov/reference-library/handbooks/moisture/mhb-ch2.pdf> pp 2.1–2.7
- [5] Hewlett-Packard 1994 *HP 4291A RF Impedance/Material Analyzer Operating Manual Set* (Japan: Hewlett-Packard) pp 11.3–11.17
- [6] Burden B 1998 Working instructions for air-oven methods *WI No: AO1–10* (Kansas City, MO: USDA-GIPSA-TSD)
- [7] Mathsoft Inc 2001 *Mathcad User's Guide with Reference Manual—Mathcad 2001i* (Cambridge, MA: Mathsoft)
- [8] Mongia R , Bahl I and Bhartia P 1999 Special representation of two-port networks *RF and Microwave Coupled-Line Circuits* (Norwood, MA: Artech House) pp 47–56
- [9] Gillay Z and Funk D B 2003 Sensitivity analysis for VHF dielectric grain moisture measurements *ASAE Paper* No. 033136 (St Joseph, MI: ASAE)
- [10] Mongia R , Bahl I and Bhartia P 1999 Quasi-TEM Modes *RF and Microwave Coupled-Line Circuits* (Norwood, MA: Artech House) pp 71–3
- [11] NIST 2005 Sec. 5.56.(a) Grain Moisture Meters *NIST Handbook 44—Specifications, Tolerances, and Other Technical Requirements for Weighing and Measuring Devices* ed T Butcher (Washington, DC: US Government Printing Office) pp 5.21–5.27
- [12] Hartyani P *et al* 2006 Comparison of loading methods in VHF-UGMA grain moisture measurement *MSc Thesis* Corvinus University of Budapest, Faculty of Food Science (in Hungarian)